THE JOURNAL OF PHYSICAL CHEMISTRY B

Article

pubs.acs.org/JPCB

On the Cis to Trans Isomerization of Prolyl−Peptide Bonds under Tension

Jian Chen,[†] Scott A. Edwards,[‡,†] Frauke Gräter,*[,§,†] and Carsten Baldauf*[,∥,†]

[†]CAS-MPG Partner Institute and Key Laboratory for Computational Biology (PICB), 320 Yue Yang Road, Shanghai 200031, China,

[‡]College of Physics and Technology, Shenzhen University, Shenzhen 518060, Guangdong, China,

[§]Heidelberg Institute for Theoretical Studies, Schloss-Wolfsbrunnenweg 35, D-69118 Heidelberg, Germany, and

[∥]Fritz-Haber-Institut der Max-Planck-Gesellschaft, Faradayweg 4-6, D-14195 Berlin-Dahlem, Germany

Supporting Information

ABSTRACT: The cis peptide bond is a characteristic feature of turns in protein structures and can play the role of a hinge in protein folding. Such cis conformations are most commonly found at peptide bonds immediately preceding proline residues, as the cis and trans states for such bonds are close in energy. However, isomerization over the high rotational barrier is slow. In this study, we investigate how mechanical force accelerates the cis to trans isomerization of the prolyl−peptide bond in a stretched backbone. We employ hybrid quantum mechanical/molecular mechanical force-clamp molecular dynamics simulations in order to describe the electronic effects involved. Under tension, the bond order of the prolyl−peptide bond decreases from a partially double toward a single bond, involving a reduction in the electronic conjugation around the peptide bond. The conformational change from cis to extended trans takes place within a few femtoseconds through a nonplanar state of the nitrogen of the peptide moiety in the transition state region, whereupon the partial double-bond character and planarity of the peptide bond in the final trans state is restored. Our findings give insight into how prolyl−peptide bonds might act as force-modulated mechanical timers or switches in the refolding of proteins.

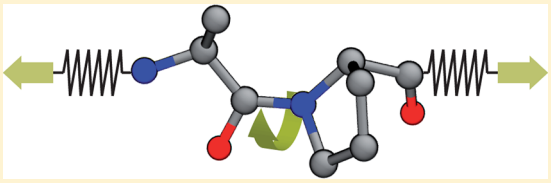

INTRODUCTION

The imino acid proline is unique among the proteinogenic amino acids, as the side chain is linked back to the backbone via a bond to the nitrogen, making it a secondary amine. This feature is the basis for a number of distinctive structural characteristics of proline in the context of peptide sequences: (i) the lack of a polar hydrogen prohibits proline from acting as a H-bond donor; (ii) the backbone torsion angle ϕ (angle $CNC_\alpha C$) is part of the heterocycle and thus conformationally restricted; and (iii) the trans state of the prolyl peptide bond is energetically only slightly preferred over the cis state, as in either case the C_β of the preceding residue is close to a carbon atom of proline (either C_α or C_δ). This is reflected in the analysis of high-resolution X-ray structures from the RCSB protein data bank,[1] where more than 90% of the cis peptide bonds in proteins are Xaa-Pro imide bonds.[2] Still, the barrier between both states is high, and the interconversion from cis to trans is slow in equilibrium.[3−6] The general mechanism of peptide bond isomerization involves a change of the bond order from a partial double bond to a single bond, followed by a return to partial double-bond character. This is caused by the pyrrolidine N changing from a planar sp^2 state to a pyramidal sp^3 state with a lone pair orbital. The resulting lone pair dipole interacts with the C═O dipole and influences the peptide bond rotation during isomerization.[7] Furthermore, the transition state is stabilized by the interaction between the N−H of the following peptide bond with the lone pair of the sp^3 N.[5,8] This isomerization can be catalyzed by peptidyl−prolyl cis−trans isomerases.[9−12]

Proline is found in a number of structural proteins, including tropoelastin. Elastin-like polypeptides (ELP) are models of tropoelastin and consist of multiple repeats of the sequence Val-Pro-Gly-Xaa-Gly. The high Pro content results in a high share of cis-prolyl peptide bonds. Single-molecule force-spectroscopy experiments by Zauscher and co-workers on ELP and poly-Pro peptides revealed a temperature-independent extensional transition upon application of a stretching force. This increase of the contour length was interpreted as force-induced cis to trans isomerization of multiple prolyl−peptide bonds.[13] A scheme of the cis to trans isomerization is shown in Figure 1A.

Another place where cis peptide bonds and Pro residues are frequently found in proteins is at type VI β turns, with a cis prolyl−peptide bond between residues 2 and 3 of the turn.[14,15] Such turns act as hinges during protein folding and arrange helices and strands in their native three-dimensional fold. The structural difference between the cis and the trans conformation of the peptide bond is significant, and an isomerization might substantially alter protein (re)folding pathways and timings.[6] An example where mechanical force meets the regulation of

Received: May 3, 2012
Revised: July 4, 2012
Published: July 6, 2012

   dx.doi.org/10.1021/jp3042846 | J. Phys. Chem. B 2012, 116, 9346−9351

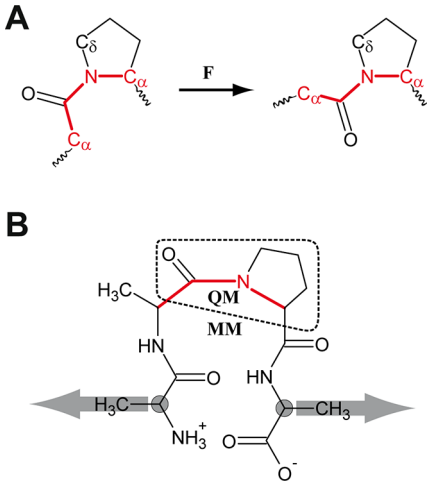

Figure 1. (A) Schematic representation of the cis to trans isomerization. Bonds and atoms defining the peptide bond torsion are highlighted in red. (B) Schematic representation of the AAPA peptide as modeled in our simulations. QM region is separated from the MM region by a dashed line. In the force-clamp simulations, the C_α atoms of Ala1 and Ala4 (gray spheres) were subjected to a constant force in opposite directions.

physiological function is the giant blood protein von Willebrand factor (VWF). The multimers of VWF are sensitive to the shear forces present in flowing blood and translate shear flow to an extensional force along its length axis.[16,17] As a result, individual domains of VWF partially unfold and eventually βVIa turns with cis prolyl−peptide bonds are under direct extensional force. Possible refolding is hindered if the prolyl−peptide bond of the βVIa turn isomerizes to the trans form.[18] Indeed, in a subset of the optical tweezers experiments reported by Springer and co-workers refolding of the tethered A2 was delayed.[19] This can be interpreted as force-induced cis to trans isomerization of the prolyl−peptide bond in the A2 domain that hampers refolding.

The question arises how mechanical force facilitates the prolyl cis to trans interconversion over the rotational barrier of 60−80 kJ/mol.[5,8] Because of a general interest in mechanochemistry and with regard to the potential physiological importance of this process, we present here a study of the forced cis to trans isomerization of the prolyl−peptide bond by classical molecular mechanics and hybrid quantum mechanics/molecular mechanics (QM/MM) force-clamp molecular dynamics (FCMD) simulations. Previous theoretical efforts to reveal the mechanism of isomerization have employed optimizations along the reaction pathway from trans to cis, based on a QM or QM/MM description.[5,7,8,20] We obtained dynamic trajectories and kinetic information as a function of the applied external force while also taking full solvation into account. We find mechanical stretching of the peptide to weaken the peptide bond, making the distorted nonplanar transition state region with reduced electronic delocalization accessible within shorter time scales.

RESULTS AND DISCUSSION

To trigger the isomerization transition from cis to trans prolyl−peptide bond, we applied an extensional force to the backbone of a short model peptide, AAPA (Figure 1B), dissolved in water during FCMD simulations. The C_α of residues Ala1 and Ala4 were subjected to a constant pulling force (Figure 1B). In response to the applied force, AAPA adopted an extended configuration, with the prolyl−peptide bond maintaining its cis conformation.

Starting from this mechanically stretched peptide conformation, we next investigated the isomerization reaction of the prolyl peptide bond in AAPA. The cis to trans isomerization reaction under force can be expected to require a change of bond character and hybridization of the involved atoms. These electronic structure effects are not accurately described by classical force fields, which are parametrized on the basis of equilibrium states without considering transition states. We therefore relied on hybrid quantum mechanical and molecular mechanical simulations (QM/MM) to consider electronic effects relating to the prolyl−peptide bond (Figure 1B). Constant forces ranging from 1.1 to 5 nN were applied; the lowest force for which isomerization was observed within a time of 500 ps was 3 nN. The experiments of Valiev et al. on ELP were performed with a constant pulling velocity; the forces they measured prior to the isomerization event were lower than ours by a factor of 10, in the range of 200−260 pN.[13] Higher forces induced isomerization on shorter time scales, with a subpicosecond transition in the 4−5 nN range (Figure 2). The force

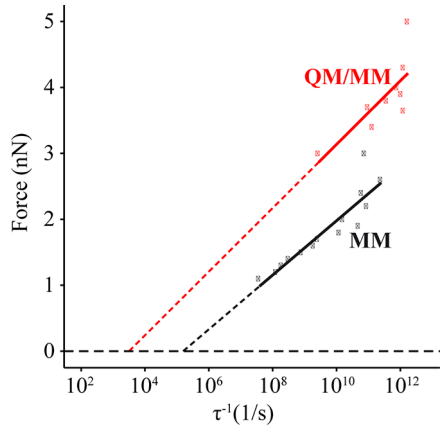

Figure 2. Isomerization lifetimes τ at different forces as obtained from FCMD simulations. Lifetimes from QM/MM simulations are shown in red and those from pure MM simulations in black. Fits of the linear Bell model[21] to the data are shown as lines.

dependence of the transition time was fitted with the linear Bell model,[21,22] yielding a distance Δx of 0.02 ± 0.007 nm between the reactant (cis) state and the transition state. The model predicts a lifetime at zero force (and similarly at the relatively low forces in experiments[13]) on the order of $\tau_0 \approx 10^{-4}$ s. However, the limited range of time scales accessible in the QM/MM simulations entails a large uncertainty of these values and does not allow us to distinguish between linear (like the Bell model) and nonlinear models like the Dudko−Hummer model.[23] Nevertheless, our simulations can be semiquantitatively validated by comparison to experiment. Using the Eyring equation, the estimated lifetime can be converted into an activation free energy of ∼60 kJ/mol, which is in line with the experimental zero force barrier of ∼60−80 kJ/mol.[13,24−26] The barrier appears indeed slightly underestimated, as we predict life times on the order of 0.1 ms instead of the lifetimes in atomic force microscopy experiments, which are larger than milliseconds.[13] However, the overall agreement is satisfying given the difference in force application (here constant force, in

dx.doi.org/10.1021/jp3042846 | J. Phys. Chem. B 2012, 116, 9346−9351

experiments constant velocity pulling) and the limited time scales of our simulations necessitating a defective extrapolation.

At a first glance, performing the same FCMD simulations of the AAPA peptide in a pure MM description appears to reproduce the main findings of the QM/MM simulations (Figure 2). Indeed, a similar linear dependency of the logarithm of the lifetime of the cis isomer to the applied force was observed, now spanning a larger force and time range. The Bell model fit gives $\Delta x = 0.023 \pm 0.004$ nm, comparable to the value obtained from our QM/MM simulations. However, for a given lifetime, smaller forces are required in the MM simulations as compared to QM/MM, as reflected by a shorter zero-force lifetime of $\tau_0 \approx 10^{-5}$ s. Even with an error of at least 1 order of magnitude up or down, we can conclude that the MM description underestimates the transition free energy barrier for isomerization. As we will show further below, this is due to the lack of changes in hybridization and bond order during the process.

How does the cis to trans isomerization proceed? We next analyze the mechanism of the isomerization via geometrical properties of the model system. In the following we will focus on the QM/MM trajectory at 3 nN, the lowest force for which isomerization was observed on accessible time scales. The macroscopic order parameter observed in pulling experiments with optical tweezers or atomic force microscopy is an increase of the contour length, which here corresponds to the distance $d_{C\alpha C\alpha}$ of the C_α atoms adjacent to the prolyl−peptide bond. During the simulation a sudden jump of $d_{C\alpha C\alpha}$ from about 0.35 to roughly 0.4 nm can be observed between 360 and 370 ps of simulation time (Figure 3A), which indicates a two-step process. The resulting difference between the stretched cis and trans states is 0.05 nm; the difference between the equilibrium cis state and the stretched trans state is about 0.1 nm, well in line with an investigation by Reimer and Fischer, who measured C_α distances around Pro residues of selected X-ray structures from the Protein Data Bank. For residues directly adjacent to the Pro residue, they reported an increase in $d_{C\alpha C\alpha}$ from cis to trans of about 0.08 nm.[27] The change in prolyl peptide bond geometry between the two isomers translates into larger shifts in the adjacent backbone segments. This is why Valiev et al. consider an increase of the contour length by 0.2 nm per cis to trans isomerized prolyl−peptide bond as an effect on the overall peptide conformation.[13] Simultaneously with the increase in contour length, the dihedral angle $\omega_{Ala-Pro}$ (defined by the backbone atoms C_α−C−N−C_α) rotates from 0° (cis) to 180° (trans) (Figure 3B). This behavior confirms that experimental observations of jumps in contour length during the stretching of ELP[13,28] and VWF[29,19] can be interpreted as prolyl−peptide bond isomerization into the trans state.

The C_α distance corresponds to the experimental observables, yet it offers only limited insight into the mechanism of isomerization. Thus, we focus on further order parameters describing the transition mechanism. One such parameter is the bond length d_{CN} of the peptide bond, which is plotted in Figure 3C. In equilibrium, the C−N peptide bond is shorter than a typical single C−N bond, as the p orbitals of N and carboxyl C are conjugated. The single peak of d_{CN} from 0.14 to 0.145 nm and back coincides with the jumps in contour length and peptide bond torsion angle. This illustrates that the change of bond order from partially double to single and back is a consequence of the elimination of orbital conjugation and its reformation between C and N. The connected change in hybridization state of the peptide bond N can be tracked by the

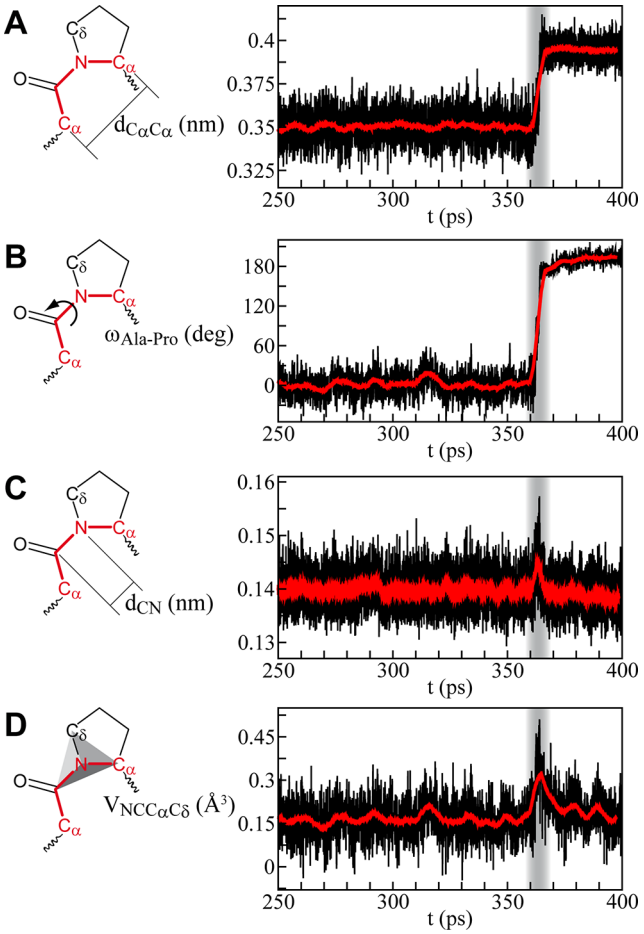

Figure 3. Mechanism of a cis to trans isomerization event (QM/MM, $F = 3$ nN). Different order parameters are shown with respect to the simulation time: (A) contour length given by the distance between the C_α atoms of Ala2 and Pro3 ($d_{C\alpha C\alpha}$); (B) torsion angle of the peptide bond between Ala2 and Pro3 ($\omega_{Ala-Pro}$); (C) length of the peptide bond between Ala2 and Pro3 (d_{CN}); (D) volume $V_{NCC\alpha C\delta}$ of the tetrahedron defined by the atoms C (of Ala2), N, C_α, and C_δ (of Pro3) as a measure for N hybridization. Black lines show the measured values from the FCMD simulation; red lines are running averages with a window size of 100 data points. Time range of isomerization is highlighted by gray rectangles.

volume of the tetrahedron consisting of the nitrogen and the atoms bound to it (C, C_α, C_δ) as shown in Figure 3D. In the stretched cis state, the pyramid N, C, C_α, C_δ has a volume of 0.15 Å^3. During isomerization, this volume peaks at 0.3 Å^3 and relaxes back to about 0.15 Å^3 (Figure 3D) following the transition of the N hybridization from sp^2 to sp^3 and back to sp^2.

The force-induced cis to trans isomerization of the prolyl−peptide bond occurs through a rotation of the peptide bond torsion angle by roughly 100° (Figure 4A). According to an overview of the possible transition states by Fischer,[30] this transition state can be characterized as syn/exo. Only the Ala2-Pro3 peptide bond rotates, while the other torsions have been already stretched out by the pulling force and remain at extended values around 180° (except the ϕ_{Pro3} which is fixed in the heterocycle). The transition state can be more readily analyzed by relating the major order parameter, the prolyl dihedral angle ω, to the other degrees of freedom affected by the isomerization, namely, $d_{C\alpha C\alpha}$, d_{CN}, and $V_{NCC\alpha C\delta}$ (Figure

dx.doi.org/10.1021/jp3042846 | J. Phys. Chem. B 2012, 116, 9346−9351

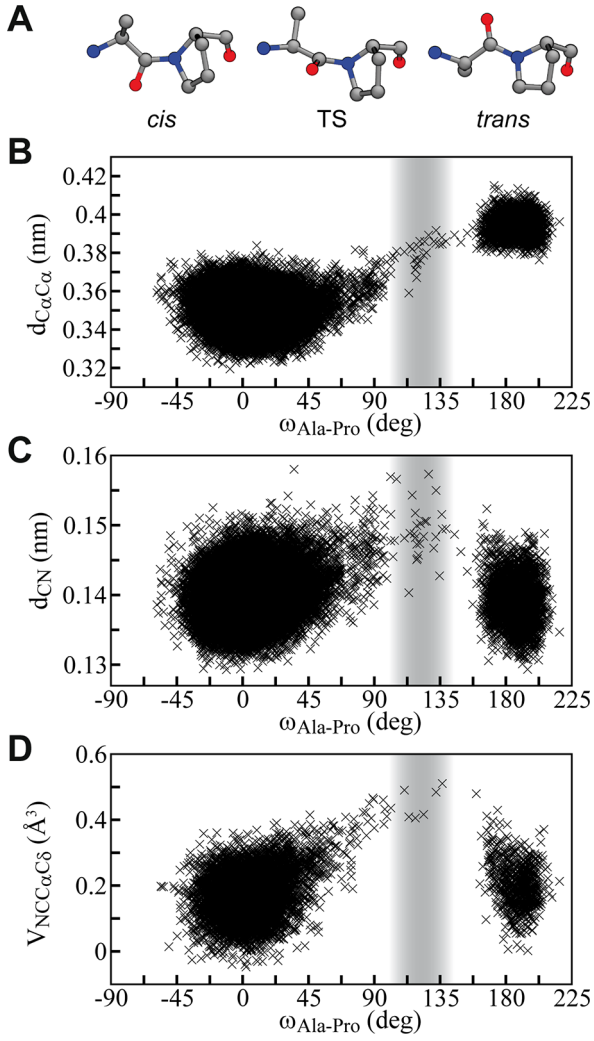

Figure 4. (A) Representative snapshots from the QM/MM trajectory at F = 3 nN, exemplifying cis, transition (TS), and trans state. (B) Distance of C_α atoms of Ala2 and Pro3 ($d_{C\alpha C\alpha}$) plotted versus the torsion angle of the peptide bond between Ala2 and Pro3 ($\omega_{Ala-Pro}$). (C) Length of the peptide bond between Ala2 and Pro3 (d_{CN}) plotted versus $\omega_{Ala-Pro}$. (D) Volume $V_{NCC\alpha C\delta}$ of the tetrahedron defined by the atoms C (of Ala2), N, C_α, and C_δ (of Pro3) plotted versus $\omega_{Ala-Pro}$.

4B–D). The change in peptide bond torsion angle $\omega_{Ala-Pro}$ coincides with the change in contour length measured by $d_{C\alpha C\alpha}$ in Figure 4B. Even though our force-clamp MD simulations do not allow us to draw quantitative conclusions on the transition state, Figure 4B clearly features an area with a low population of states (gray shade), within which the transition state is likely to be located. Notably, this transition state region features an angle $\omega \geq 100°$, slightly beyond the halfway rotation, and a contour length $d_{C\alpha C\alpha}$ between 0.36 and 0.39 nm. This corresponds to an elongation with respect to the product state by 0.01–0.04 nm. Thus, the change in contour length from the cis to the ~100° rotated state serves as a direct structural interpretation of the Δx of 0.02 ± 0.007 nm obtained from the Bell model fit (see above) and suggests this as the transition state. Both the peptide bond length (d_{CN}) and $V_{NCC\alpha C\delta}$ only show increased values within the sparsely populated region of conformational space that includes the transition state and then return to equilibrium values (Figure 4C and 4D). Again, this highlights the change in bond character (double to single and back to double) and hybridization (sp^2 to sp^3 and back to sp^2) during isomerization. In all our simulations, employing a range of different forces, isomerization occurs by rotation from 0° via 90° to 180°, with the lone pair of the sp^3 passing an ecliptic conformation with the preceding C_α. Rotation via −90°, with an ecliptic orientation of the lone pair and the carboxyl O, was never observed. In a previous theoretical study of the isomerization in the absence of mechanical strain both rotation directions were observed.[8] Another important feature of the mechanism shown in previous studies is that the pyramidal state of the peptide bond N is stabilized by a N···H interaction with a downstream backbone NH.[5,8] Here, instead, activation of the prolyl–peptide bond is not promoted by an attacking nucleophile but by mechanical force.

How can the described force-induced isomerization mechanism (Figure 4) be related to the increase in rate (Figure 2)? Forces of a few nN extend the C–N bond to a length that is closer to the single bond (0.147 nm) than to the double bond (0.132 nm). This change in length of the C–N bond in the cis and trans state as well as for the transition state region is shown in Supporting Information Figure 2 for the sampled range of forces. The transition state region features bond lengths typical of a single bond, while the product trans state relaxes back to partial double-bond character. Stress relief after isomerization allows bond lengths even smaller than that of the cis state at the same force. Thus, application of mechanical force destabilizes the reactant cis state, thereby moving it closer to the transition state. It may be that a stabilization of the transition state by force is another factor for lowering the activation barrier, but the limited sampling of transitions does not allow the inference of a relationship between the transition state energy of bond character and force (Supporting Information Figure 2).

From a technical point of view, it is interesting to compare the mechanism of isomerization as observed in the QM/MM description with the pure OPLS-AA force field treatment. In both setups, sudden and concurrent changes of the contour length and the peptide bond torsion angle, the two main order parameters representing the peptide bond isomerization, can be observed (Figure 3 and Supporting Information Figure 3). A clear difference becomes obvious when monitoring d_{CN} and $V_{NCC\alpha C\delta}$. The isomerization mechanism involves transient femtosecond scale changes in both parameters with the QM/MM treatment (Figure 3), whereas no such changes occur in the classical force field model (Supporting Information Figure 3). In the pure MM treatment, the force constant of the prolyl peptide bond potential remains unmodified and cannot reflect the bond order changes of the peptide bond undergoing isomerization. Furthermore, the change of the hybridization state of the nitrogen, measured via the tetrahedron volume $V_{NCC\alpha C\delta}$, is prevented by the improper dihedral potentials exerted on the peptide bond in the force field description of the system. Thus, as expected, only the QM/MM simulation is able to reflect the nature of the isomerization of the prolyl–peptide bond, most importantly including the transient sp^3 hybridization of N associated with a loss of π-electron conjugation of the prolyl–peptide bond.

■ CONCLUSION

In this work, we were able to elucidate the mechanism of force-induced cis to trans isomerization of the prolyl–peptide bond with QM/MM FCMD simulations. Tensile force releases the partial double bond and converts it to a single bond, rather like

dx.doi.org/10.1021/jp3042846 | J. Phys. Chem. B 2012, 116, 9346–9351

a clutch. Isomerization (rotation around the peptide bond) can then occur, and afterward the 'clutch' closes and the partial double bond reforms. In quantitative agreement with experiments, force increases the isomerization rate. One important factor for the force-induced acceleration is a lengthening of the reactive C−N bond by force toward the single-bond character of the transition state.

A previously discussed mechanism for the cis to trans isomerization in equilibrium by Karplus and co-workers is based on the interaction of a downstream amide hydrogen with the free electron pair of the transition state nitrogen.[5,8] Such a mechanism is impossible in the stretched state of the peptide under tensile force. Instead, force appears to take up the role of the activating stimulus and stabilizes the transition state (the change of bond order and hybridization) which allows for isomerization. Another interesting observation of our study is that the direction of the isomerization always proceeds from 0° via 90° to 180°. Apparently, the chirality of the peptide in combination with the strain along its length axis results in a preferred rotation direction. The semiquantitative agreement of our MM and QM/MM simulations on the lifetime−force relation is of methodological interest. However, the limitations of molecular mechanics become obvious when studying the actual isomerization mechanism whose main features, the changes of the bond order and the hybridization state, can only be accounted for by electronic structure theory.

Our study demonstrates that cis to trans isomerization can be triggered by mechanical force. It contributes to an interpretation of experimental findings on the behavior of ELP under tensile force.[13] Our findings are of special relevance to the purported regulatory role played by force-triggered cis to trans isomerization of the prolyl−peptide bond, in which it acts as a folding timer: in force-responsive proteins, cis prolyl−peptide bonds can isomerize to the trans state and hinder refolding until spontaneous isomerization returns it to the original state. We note that our results suggest only a minor acceleration of the cis to trans isomerization (by a factor of less than 10) at physiological forces of less than a few 100 pN. Nevertheless, if isomerization is a rate-limiting step for protein folding, tensile forces can tune the competition between proline isomerization and folding, thereby potentially altering folding pathways. We speculate that such a mechanism may be functionally important for the blood protein VWF.

METHODS

The tetrameric peptide Ala1-Ala2-Pro3-Ala4 (AAPA) was modeled in a type VIa β-turn conformation and immersed within a cubic TIP4P[31] water box. Classical MM MD simulations were performed with Gromacs 3.3.1[32] and the OPLS-AA force field,[33] with an MD step size of 2 fs. Cut offs were applied to van der Waals interactions, and the particle-mesh Ewald method was used for long-range electrostatics.[34] The simulations were carried out in an NPT ensemble coupling to a Nosé−Hoover thermostat[35,36] of 300 K and to a Parinello−Rahman barostat of 1 atm.[37] The initial system was prepared by performing a free MD simulation in equilibrium for 50 ns. Later, external stretching force was applied to the C_α atoms of residues Ala1 and Ala4 (highlighted in Figure 1B). A series of FCMD simulations[38] was performed with constant forces ranging from 0.1 to 3 nN; a list with all forces for which cis to trans isomerization occurred can be found in Supporting Information Table S1.

The combined QM/MM simulations under tension were performed with Gromacs-3.3.1[32] and Gaussian03.[39] As shown in Figure 1B, the tetrapeptide AAPA was divided into a QM region and a MM region by cutting the carbon−carbon bonds, as the dashed line shows. The QM region with 16 atoms was simulated with B3LYP/6-31G* hybrid density functional theory[40,41] as implemented in Gaussian03. The carbon−carbon bonds connecting the QM and MM part were capped with hydrogens for QM calculations.[42,43] The QM part of the system was modeled under a Coulomb field of all MM atoms. The QM/MM FCMD simulations were carried out with constant forces from 2 to 5 nN with an integration step size of 1 fs, starting from a structure sampled from MM simulations at the same force.

ASSOCIATED CONTENT

Supporting Information

Details of the simulation setups and results of the equilibrium MD and pure MM FCMD simulations; brief analysis of the pure MM equilibration MD simulation of AAPA; tables with the lifetimes of cis states in pure MM and QM/MM FCMD simulations; plot with d_{CN} bond distances of the prolyl peptide bond in the cis, trans, and transition state over a range of applied forces; order parameters $d_{C\alpha C\alpha}$, $\omega_{Ala-Pro}$, d_{CN}, and $V_{NCC\alpha C\delta}$ of the prolyl peptide bond from a pure MM FCMD simulation; exemplary structure files of the initial conformation, extended cis conformation, and extended trans conformation of Ala-Ala-Pro-Ala. This material is available free of charge via the Internet at http://pubs.acs.org.

AUTHOR INFORMATION

Corresponding Author

*E-mail: frauke.graeter@h-its.org; baldauf@fhi-berlin.mpg.de.

Notes

The authors declare no competing financial interest.

ACKNOWLEDGMENTS

Support by Gerrit Groenhof (Göttingen) for realization of the QM/MM scheme is gratefully acknowledged. C.B. thanks Hans-Jörg Hofmann (Leipzig) for his comments on the manuscript. The authors thank the Klaus Tschira foundation for financial support. J.C. acknowledges support by the Postdoctoral Research Program of the Shanghai Institutes for the Biological Sciences, Chinese Academy of Sciences (2011KIP514). F.G. and C.B. acknowledge funding from Deutsche Forschungsgemeinschaft (Forschergruppe 1543: Shear flow regulation in hemostasis−Bridging the gap between nanomechanics and clinical presentation), and F.G. acknowledges funding from the DAAD (Sino-German Junior Research Group for Biotechnology). S.A.E. acknowledges support from the Max Planck Society, a CAS Young International Scientist Fellowship (O91GC11401), and an NSFC Research Fellowship for International Young Scientists (O93DC11401).

REFERENCES

(1) Berman, H.; Westbrook, J.; Feng, Z.; Gilliland, G.; Bhat, T.; Weissig, H.; Shindyalov, I.; Bourne, P. *Nucleic Acids Res.* **2000**, *28*, 235−242.
(2) Weiss, M.; Jabs, A.; Hilgenfeld, R. *Nat. Struct. Mol. Biol.* **1998**, *5*, 676−676.
(3) Salahuddin, A. *J. Biosci.* **1984**, *6*, 349−355.
(4) Stewart, D.; Sarkar, A.; Wampler, J. *J. Mol. Biol.* **1990**, *214*, 253−260.

(5) Fischer, S.; Dunbrack, R. L.; Karplus, M. *J. Am. Chem. Soc.* **1994**, *116*, 11931−11937.
(6) Wedemeyer, W.; Welker, E.; Scheraga, H. *Biochemistry* **2002**, *41*, 14637−14644.
(7) Wiberg, K. B.; Laidig, K. E. *J. Am. Chem. Soc.* **1987**, *109*, 5935−5943.
(8) Yonezawa, Y.; Nakata, K.; Sakakura, K.; Takada, T.; Nakamura, H. *J. Am. Chem. Soc.* **2009**, *131*, 4535−4540.
(9) Gothel, S.; Marahiel, M. *Cell. Mol. Life Sci.* **1999**, *55*, 423−436.
(10) Leuzzi, R.; Serino, L.; Scarselli, M.; Savino, S.; Fontana, M.; Monaci, E.; Taddei, A.; Fischer, G.; Rappuoli, R.; Pizza, M. *Mol. Microbiol.* **2005**, *58*, 669−681.
(11) Siegrist, R.; Zürcher, M.; Baumgartner, C.; Seiler, P.; Diederich, F.; Daum, S.; Fischer, G.; Klein, C.; Dangl, M.; Schwaiger, M. *Helv. Chim. Acta* **2007**, *90*, 217−259.
(12) Braun, M.; Hessamian-Alinejad, A.; De Lacroix, B.; Alvarez, B.; Fischer, G. *Molecules* **2008**, *13*, 995−1003.
(13) Valiaev, A.; Lim, D.; Oas, T.; Chilkoti, A.; Zauscher, S. *J. Am. Chem. Soc.* **2007**, *129*, 6491−6497.
(14) Hutchinson, E. G.; Thornton, J. M. *Protein Sci.* **1994**, *3*, 2207−2216.
(15) Möhle, K.; Gußmann, M.; Hofmann, H. *J. Comput. Chem.* **1997**, *18*, 1415−1430.
(16) Alexander-Katz, A.; Schneider, M. F.; Schneider, S. W.; Wixforth, A.; Netz, R. R. *Phys. Rev. Lett.* **2006**, *97*, 138101.
(17) Schneider, S. W.; Nuschele, S.; Wixforth, A.; Gorzelanny, C.; Alexander-Katz, A.; Netz, R. R.; Schneider, M. F. *Proc. Natl. Acad. Sci. U.S.A* **2007**, *104*, 7899−7903.
(18) Baldauf, C.; Schneppenheim, R.; Stacklies, W.; Obser, T.; Pieconka, A.; Schneppenheim, S.; Budde, U.; Zhou, J.; Gräter, F. *J. Thromb. Haemost.* **2009**, *7*, 2096−2105.
(19) Zhang, X.; Halvorsen, K.; Zhang, C.; Wong, W.; Springer, T. *Science* **2009**, *324*, 1330.
(20) Fischer, S.; Michnick, S.; Karplus, M. *Biochemistry* **1993**, *32*, 13830−13837.
(21) Bell, G. I. *Science* **1978**, *200*, 618−627.
(22) Evans, E.; Ritchie, K. *Biophys. J.* **1997**, *72*, 1541−1555.
(23) Dudko, O.; Hummer, G.; Szabo, A. *Phys. Rev. Lett.* **2006**, *96*, 108101.
(24) Fischer, G.; Schmid, F. X. *Biochemistry* **1990**, *29*, 2205−2212.
(25) Dugave, C.; Demange, L. *Chem. Rev.* **2003**, *103*, 2475−2532.
(26) Aliev, A.; Bhandal, S.; Murias, D. C. *J. Phys. Chem. A* **2009**, *113*, 10858−10865.
(27) Reimer, U.; Fischer, G. *Biophys. Chem.* **2002**, *96*, 203−212.
(28) Valiaev, A.; Lim, D.; Schmidler, S.; Clark, R.; Chilkoti, A.; Zauscher, S. *J. Am. Chem. Soc.* **2008**, *130*, 10939−10946.
(29) Springer, T. A. *J. Thromb. Haemost.* **2011**, *9*, 130−143.
(30) Fischer, G. *Chem. Soc. Rev.* **2000**, *29*, 119−127.
(31) Jorgensen, W.; Jenson, C. *J. Comput. Chem.* **1998**, *19*, 1179−1186.
(32) Lindahl, E.; Hess, B.; van der Spoel, D. *J. Mol. Model.* **2001**, *7*, 306−317.
(33) Jorgensen, W.; Ulmschneider, J.; Tirado-Rives, J. *J. Phys. Chem. B* **2004**, *108*, 16264−16270.
(34) Darden, T.; York, D.; Pedersen, L. *J. Chem. Phys.* **1993**, *98*, 10089−10092.
(35) Hoover, W. *Phys. Rev. A* **1985**, *31*, 1695.
(36) Nose, S. *Mol. Phys.* **1984**, *52*, 255−268.
(37) Parrinello, M.; Rahman, A. *J. Appl. Phys.* **1981**, *52*, 7182−7190.
(38) Grubmüller, H.; Heymann, B.; Tavan, P. *Science* **1996**, *271*, 997.
(39) Frisch, M. J.; et al. *Gaussian 03*, Revision C.02; Gaussian, Inc.: Wallingford, CT, 2004.
(40) Becke, A. *J. Chem. Phys.* **1993**, *98*, 5648−5652.
(41) Lee, C.; Yang, W.; Parr, R. *Phys. Rev. B* **1988**, *37*, 785.
(42) Field, M.; Bash, P.; Karplus, M. *J. Comput. Chem.* **1990**, *11*, 700−733.
(43) Groenhof, G.; Bouxin-Cademartory, M.; Hess, B.; de Visser, S. P.; Berendsen, H. J. C.; Olivucci, M.; Mark, A. E.; Robb, M. A. *J. Am. Chem. Soc.* **2004**, *126*, 4228−4233.